FTD-TT- 63-159

6332

TRANSLATION

NEWS OF THE INSTITUTES OF HIGHER LEARNING: AERONAUTICAL ENGINEERING (SELECTED ARTICLES)

FOREIGN TECHNOLOGY DIVISION

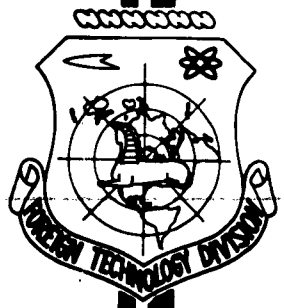

AIR FORCE SYSTEMS COMMAND

WRIGHT-PATTERSON AIR FORCE BASE

OHIO

402471

UNEDITED ROUGH DRAFT TRANSLATION

NEWS OF THE INSTITUTES OF HIGHER LEARNING: AERONAUTICAL ENGINEERING (SELECTED ARTICLES)

English Pages: 29

Source: Russian periodical: Izvestiya VUZov, Aviatsionnaya Tekhnika, No. 2, 1962. pp. 102-112, 159-167.

SOV/147-62-0-2

PREPARED BY:

TRANSLATION SERVICES BRANCH
FOREIGN TECHNOLOGY DIVISION
WP-AFB, OHIO.

TABLE OF CONTENTS

INVESTIGATION OF THE WORKING CASCADES OF TURBINES AT SUPERSONIC VELOCITIES

A. V. Gubarev

The possibility of developing, in a single stage of a turbine, large heat drops without a noticeable decrease in the efficiency is a very attractive idea. However, up to now there have been no reliable methods for profiling working cascades which operate with satisfactory efficiency at high supersonic velocities. In addition, up to now there have been no intense studies of working cascades at such velocities.

In this paper we present certain results of an investigation of working cascades at supersonic velocities [1]. Profiles of the working cascades, built according to the recommended methods, made it possible to noticeably increase the efficiency of certain turbines of the Kaluga factory.

1. Features of Supersonic-Flow Structure in Working Cascades and the Method of Designing New Cascades

In the literature [2] it is usually noted that at supersonic

velocities, thick leading edges of the airfoils of a cascade are the source of additional losses. However, recent studies [3, 4] have shown that under certain conditions, tapering of the leading edge does not produce the desired result. Moreover, Oswatisch [3] has established that even in the case of a knife-edge on the airfoils a complex system of head shocks forms at the cascade inlet. An analysis of the results obtained at the Moscow Power Institue [2, 5] and those obtained by other authors shows that the head shocks occurring ahead of the cascade can be divided into three groups:

1. those caused by flow past the leading edge — "edge head shocks,"

2. those that depend on the shape of the vane channel — "choking of the vane channel," and

3. those caused by an off-design flow-inlet angle — an "oblique frontal shock."

Occurring ahead of the cascade, they combine and form a complex system of head shocks; therefore they cannot be examined individually during experiments. However, such separate examination is expedient, since it would make it possible to find a way to improve working airfoil cascades designed for high supersonic velocities.

To decrease the intensity of the "edge head" shocks we must attempt to decrease the thickness and the design angle of the leading edge. However, such measures do not always make it possible to decrease the intensity of the head shocks. This is observed when a "choking" shock forms ahead of the cascade and a subsonic stream flows past the leading edges. We should mention that "edge head" shocks are local in nature, while "choking" shocks always partition off the entire flow. Therefore we can state that a great percentage of the losses

in head shocks is due to the presence of "choking" shocks.

Consequently, to decrease the losses in head shocks we must, in addition to decreasing the thickness and design angle of the leading edge, also design the vane channel of the cascade such that "choking" shocks do not occur [6].

To decrease the intensity of "oblique frontal shocks" the "effective" slope of the inlet sector of the back of the airfoil must be close to the flow-inlet angle into the cascade [5]. We should note that the problem of lowering the intensity of the head shocks at the cascade inlet should be solved complexly, since the above requirements are mutually exclusive in certain cases.

Let us examine certain features of supersonic flow in the vane channel of a cascade. We will consider that there are no head shocks and that the flow is uniform at the cascade inlet.

Since disturbances in supersonic flow are propagated only along the stream, the flow past the back of the airfoil in the inlet section will be the same as flow past an isolated body. If this part of the back of the airfoil is curvilinear, as is the case in cascades for subsonic velocities, there will be intense flow acceleration along it. Such overexpansion of the flow results in the formation of an intense compression shock and a turbulent zone about the back of the airfoil [3, 1]. According to Oswatisch [3], the losses in the turbulent zone reach 6-8%. Therefore we must exclude the possibility of flow acceleration in the inlet section of the airfoil. This problem can be solved as follows.

First method – the airfoil back in the inlet section is made with reverse concavity. This is the method of "stepwise flow stagnation."

Second method — flow stagnation in a steep shock occurring at the leading edge from the concave surface.

In both cases the vane channel is convergent-divergent, or divergent, since after the head shocks at the inlet section of the vane channel the flow is stagnant.

Supersonic cascades are usually used in stages with low volume gas passage; therefore they should be designed such that the total losses are minimum. As has been shown by studies at the Dzerzhinskiy All-Union Heat Engineering Institute and the Moscow Power Institute, for this there must be relatively low flow rates at sections of maximum curvature in the vane channel. Consequently, the terminal and airfoil losses in cascades operating at supersonic velocities can be decreased by the same method — stagnation of the flow in the initial section of the vane channel. However, the degree of stagnation of the flow, from the standpoint of lowering the total losses, can be greater than necessary to insure minimum airfoil losses.

Figure 1 shows types of airfoils designed according to recommendations. We investigated about 30 different cascades that had differing airfoil shapes, relative pitch, and angles of incidence. The table gives the basic geometric characteristics of the cascades; we will next discuss the results of their investigation.

2. Results of Investigation of the Cascades

A. Investigation of Type V Cascades

The geometric features of type V airfoils (Fig. 1a) are as follows: the thickness and design angle of the leading and trailing edges are small; the elongated sections on the airfoil back, at the flow inlet and in an oblique section, and small sectors on the convex

surface, near the edges, are straight; the curvature of the back and the convex surface near the vane channel changes smoothly.

Figure 2 gives the curves of pressure distribution along the airfoil TR-1V in cascade No. 2. The vane channel in this cascade is convergent-divergent, with its minimum cross section located at the beginning of the channel (points 7-8 and 13-14). Examination of the curves shows that with supersonic flow-inlet velocities ($M > 1$), a plane shock occurs ahead of the cascade channel; with increasing speed this shock shifts along the stream. For regimes $M > 1.5$ the head shocks enter the vane channel. In it the flow is accelerated, and at subsonic velocities in the minimum cross section its deep overexpansion is noted at the back and at the convex surface. At supersonic velocities the minimum dimensionless pressure is decreased considerably, and shifts noticeably along the flow. The intensity of the diffuser section at points 14-17 decreases.

Figure 2b gives a comparison of the pressure distribution along the airfoil in cascade No. 4 for three flow-inlet angles. The vane channel of this cascade has two narrow sections, one at the inlet and the other at the exit from the channel. After the second throat the channel expands. An examination of the curves shows that in subsoni. regimes the pressure distribution along the airfoil depends little on the flow-inlet angle. At supersonic velocities ($M = 1.45$) a change in the flow-inlet angles within the same range results in a substantial change in the pressure curves: with increasing angle, the flow velocity at the inlet section of the back of the airfoil decreases, with a simultaneous abrupt increase in the flow stagnation intensity in the compression shock.

Such a change in the pressure curves can be explained as follows:

with an increase in the flow-inlet angle ahead of the cascade there occurs an "oblique frontal shock," and the flow velocity at the inlet decreases; the increased intensity of flow stagnation at the inlet to the vane channel is caused, in turn, by the displacement of the "choking" shock against the flow, caused by decreased velocity.

Figure 3 gives the curves of the dependence of the total losses in the cascades of airfoils TR-1V and TR-2V. In the case of convergent-divergent vane channels (Fig. 3a) the maximum losses are reached at $M = 1.0$. The losses decrease in subsonic and supersonic regimes. Characteristically, maximum losses at $M = 1.0$ are found in cascade No. 1 (at $\overline{f} = 0.657$), while the minimum losses occur in cascade No. 5 (at $\overline{f} = 0.909$). This fact, and also the nature of the change of losses versus M, agree with data from Laval-nozzle studies. With increased flow-inlet angle the losses decrease throughout the entire range of velocities, which can be explained as follows: first, for large inlet angles flow stagnation occurs stepwise (in an "oblique frontal shock and, subsequently, at the leading edge and ahead of the vane channel), and second, in the investigated types of cascades the channel at the inlet is divergent, and therefore there is observed no increase in the flow-outlet angle for high M values of flow expansion in the oblique section of the cascade [5].

Figure 3b gives curves of the total losses in cascades of airfoils with a slight change in the width of the channels. This type of cascade is characterized by weak dependence of losses on Mach number. Only at $\beta_1 = 17^\circ$ (cascade No. 4) do the losses sharply increase in $M = 1.0$ regimes. Such behavior of the curves is caused by the structure of the shocks and the expansion waves at the cascade inlet. Actually, when $\beta_1 = 17^\circ$ an expansion wave forms ahead of the cascade,

since $\beta_1 < \beta_c$. The flow accelerates. Therefore, at low supersonic velocities the intensity of the "choking" shock increases considerably compared with the case $\beta_1 \geq \beta_c$, and then, for high Mach numbers, when the head shocks enter the vane channel, the losses decrease and even become somewhat smaller than for large flow-inlet angles. This can be explained by the fact that when $\beta_1 = 17^\circ$ there is no flow deviation in the oblique section.

B. Investigation of Cascades Consisting of Modified TR-1V Airfoils

To explain the influence of the geometric shape of the vane channel and the airfoil on the characteristics we investigated Cascades Nos. 6-11. The TR-1V-II airfoil differs from the TR-1V in that there is a break in the leading section of the back and in the middle cross sections of the vane channel the convex surface and the airfoil back have arcs of greater radius. There is no break in the back of the leading section of airfoil TR-1V-I.

From an examination of the spectra and also measurements of the pressure distribution along the profile we can draw the following conclusions: a) at low supersonic velocities, flow stagnation at the cascade inlet is caused by channel blockage; b) with increasing velocity the shock shifts along the flow, and only at $M \geq 1.5$ is the shock at the break in the airfoil back (Fig. 4a), i.e., the effect of stepwise flow stagnation begins to be manifested at the cascade inlet. For greater clarity, graduation lines are plotted on the airfoil surfaces; as a result, the structure of the characteristic is quite evident.

For cascades Nos. 6 and 9 it is characteristic that the minimum

section of the vane channel is at the inlet section. Main expansion of the channel occurs at the point of maximum curvature. In Fig. 4b (flow spectrum for cascade No. 9) we see the shocks in the vane channel. For a broad set of regimes (M = 1.2-1.9) the position and shape of the shocks did not change. This shock is caused by overexpansion of flow with flow past the airfoil back and by intense compression of the flow along the convex surface [5].

Figure 3c gives curves of the dependence of losses in cascades consisting of TR-1V-I, TR-1V-II, and TR-1V-2 airfoils. Since the vane channels of these cascades were divergent at the outlet, we detect the characteristic dependence of losses on Mach number: when M = 1 there are maximum losses, which then decrease considerably. For cascades Nos. 6 and 9 the calculated regimes (M = 1.6), determined from the ratio of the outlet area to the minimum area, were not reached during the experiment, and therefore the losses continually decreased with increasing velocity. We should note that when M = 0.5-1.3 the losses are greater in cascade No. 9, while when M > 1.3 the losses are higher in cascade No. 6 (by 2%); cascade No. 6 differed from No. 9 only in the absence of a break in the outlet section of the airfoil back. Consequently, stepwise stagnation is expedient at high supersonic velocities.

The high level of losses (about 17%) in cascades Nos. 7 and 10 in the calculation regimes (M = 1.45) can be explained by the fact that most intense expansion of the channel occurs before its maximum curvature. Therefore the flow at the airfoil back is overexpanded, and an intense shock occurs in the channel; as observations showed, its intensity was higher than in cascade No. 9 (see Fig. 4b). In addition, the secondary flows in this cascade were also relatively great.

In cascade No. 11 (airfoil TR-1V-2) the losses at M = 0.5-1.3 were lower than in cascades No. 6-10, which can be explained by the high value of the parameter $\bar{f}$ and the position of the maximum cross section at the outlet section of the channel. Minimum losses (about 13.5%) are attained at regimes M = 1.35-1.55, which are the calculation regimes for the given cascade.

C. Investigation of VS-Type Cascades

The geometric features of type VS airfoils (Fig. 1b) are as follows: a) a convex surface formed by an arc of a single radius; b) the design angles of the leading and trailing edges are zero. The TR-1VS-2 airfoil has a break ($\delta = 10^{\circ}$) at the inlet part of the back. The inlet sector of the vane channel is minimum and the channel diverges uniformly ($\bar{f} = 0.827$). For the TR-1VS-3 airfoil the break is decreased to 5° and the vane channel is convergent-divergent ($\bar{f} = 0.9$). The channel width is constant in a cascade consisting of TR-1VS-5 airfoils.

Figure 4c shows the flow spectrum of cascade No. 12. At low supersonic velocities we detected two head shocks: a disconnected shock, ahead of the break point on the back, and a curvilinear shock ahead of the edge. With increasing Mach number the disconnected shock becomes oblique while the curvilinear shock shifts along the flow, and in regimes greater than M = 1.5 its right branch enters the vane channel. Flow stagnation at the cascade inlet occurs in a system of oblique shocks.

Figure 3c gives curves of the total losses in VS cascades. The minimum losses in these cascades correspond to the calculation values of M for the divergent part of the channel. Characteristically, when $M > M_p$ the losses in cascade No. 13 increase only insignificantly.

Analogous behavior of the curves was also observed for cascades Nos. 10 and 11. The losses in No. 14 for $M > 1.3$ are higher than in Nos. 12 and 13.

D. Investigation of the Flow Field Behind the Cascades

Figure 5 gives certain characteristic curves of the loss distribution along the height of the cascades. In subsonic regimes, as a rule, there are intense loss peaks caused by the secondary flows. With increasing M the loss peaks decrease; however, for most of the investigated cascades the losses in the average cross section (airfoil losses) increase. This is due to boundary layer separation in transonic regimes. With a further increase in velocity ($M > 1$) most cascades are characterized by a considerable decrease of the loss peaks near the end walls and also airfoil losses. At high supersonic regimes the end losses in the cascades are very slight.

Figure 6 gives distribution curves for flow-outlet angles along the height of the cascade. With increasing M nonuniformity of flow along the height of the cascade decreases considerably, which is reflected in a decrease in the intensity of secondary flows in the cascades. We must also note that in all the investigated impulse cascades there was no flow expansion in the oblique section for regimes $M > 1$.

Conclusions

The results of systematic studies conducted at the Moscow Power Institute showed the expediency of designing three different types of working cascades: for subsonic, transonic, and supersonic velocities [7, 8]. From our work we can draw the following conclusions:

1. We have verified the developed recommendations on the design

of more effective cascades for supersonic velocities (loss levels 1.5-2-times lower). However, the loss level (13-15%) should not yet be considered satisfactory.

2. The efficiency of working cascades at transonic velocities and the calculation Mach number are determined mainly by the parameter $\overline{f} = a_{min}/a_2$.

3. In regimes $M > M_p$ the losses in the working cascades increase insignificantly, which allows us to recommend, just as for Laval nozzles, designing cascades from a calulation in order to use them in regimes greater than those calculated. However, the physical significance of these recommendations idffers from analogous ones proposed for guide cascades, since flow is not deflected in the oblique section of working cascades.

4. To decrease losses in the head shocks for high Mach numbers it is expedient to use stepwise flow stagnation.

5. For high supersonic velocities the end losses in cascades developed by the Moscow Power Institute are very slight compared with the total losses. This makes it possible to recommend the use of these cascades in the first control stages of turbines.

Department of Steam and Gas Turbines Submitted October 13, 1961

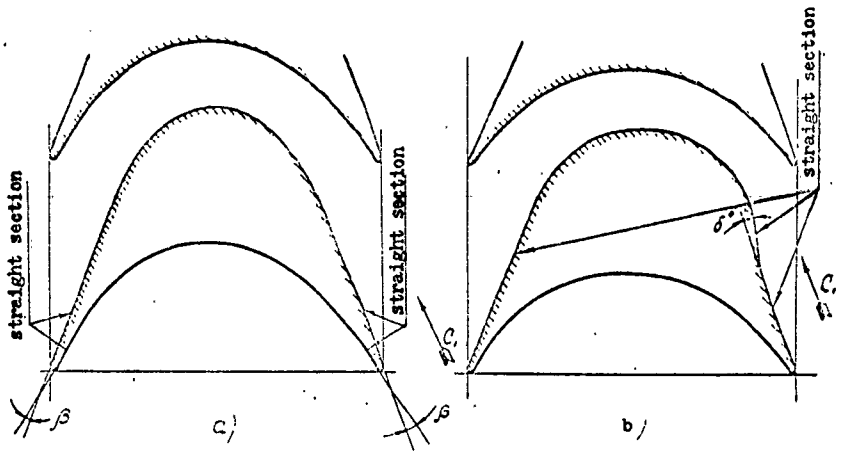

Fig. 1. Shapes of airfoils (Moscow Power Institute) for supersonic velocities: a) V-type airfoil, b) VS-type airfoil.

TABLE

Cascade number	Type of airfoil	Cord b	Relative pitch, $\bar{t}$	Angle of incidence β_{1y}	Relative height, $\bar{l}$	Effective flow outlet angle β_{2eff}	Ratio of minimum cross section to outlet cross section $\bar{f}=\frac{a_{min}}{a_2}$
1	TR-1V	20	0,525	88°51′	1,50	17°45′	0,658
2	TR-1V	20	0,575	89°05′	1,50	18°45′	0,780
3	TR-1V	20	0,500	87°51′	1,50	17°42′	0,970
4	TP-1V	15, 20, 30	0,625	88°51′	30 мм	18°52′	0,960
5	TR-2V	20	0,570	89°05′	1,50	22°25′	0,910
6	TR-1V — I	20	0,600	90°	1,50	19°00′	0,810
7	TR-1V — I	20	0,625	90°	1,50	19°20′	0,850
8	TR-1V — II*	20	0,575	89°05′	1,50	17°42′	0,800
9	TR-1V — II*	20	0,600	90°	1,50	19°00′	0,810
10	TR-1V — II*	20	0,625	90°	1,50	19°20′	0,850
11	TR-1V — 2*	20	0,625	90°	1,50	18°50′	0,920
12	TR-1VS — 2*	20	0,625	88°34′	1,50	18°25′	0,827
13	TR-1VS — 3*	20	0,625	88°34′	1,50	18°25′	0,910
14	TR-1VS — 5*	20	0,625	88°34′	1,50	18°25′	1,00

* The outlet section of the airfoil back is bent.

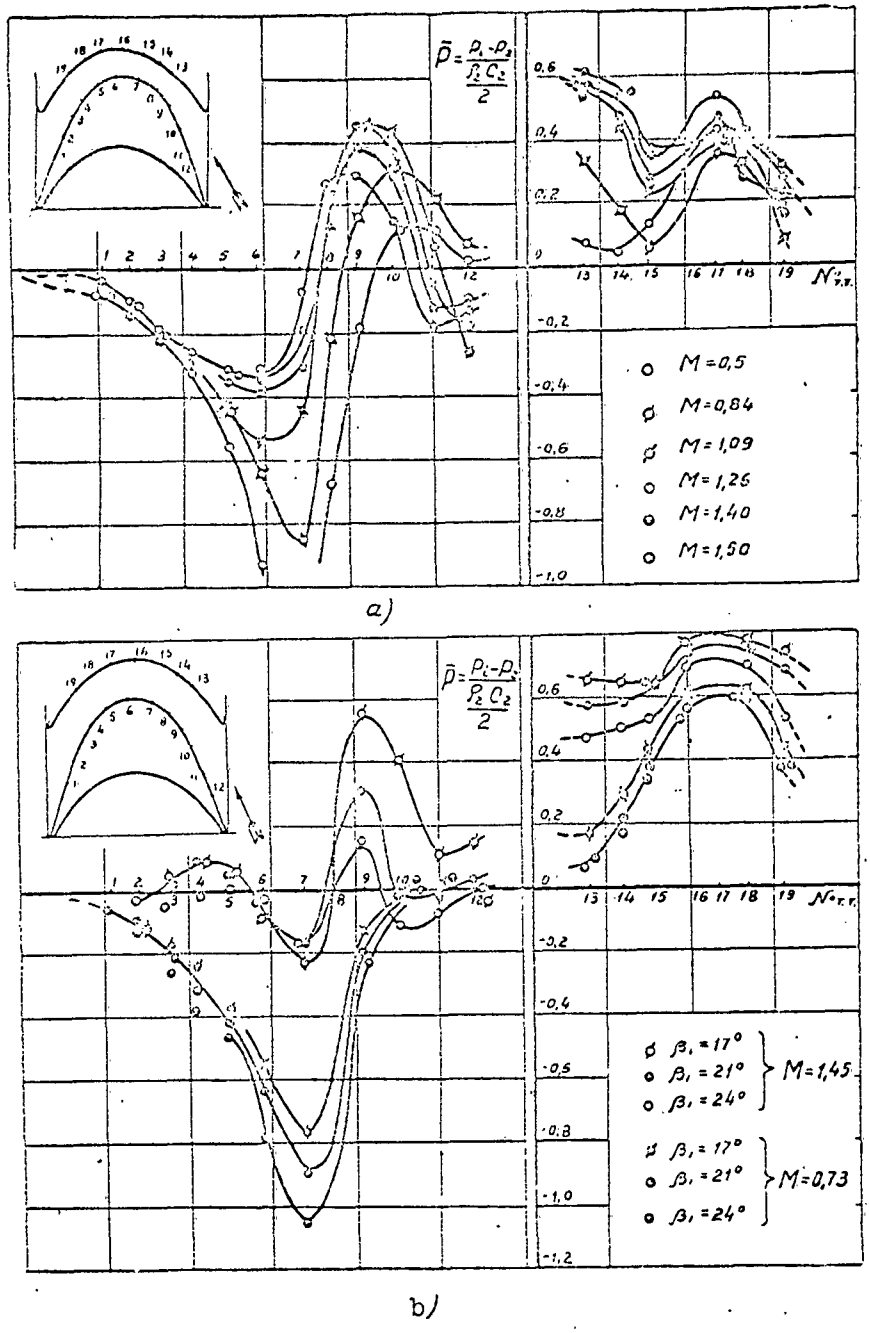

Fig. 2. Pressure distribution along the airfoil in a cascade: a) for cascade No. 2 as a function of the Mach number ($\beta_1 = 17^\circ$); b) for cascade No. 4 as a function of the flow-inlet angle.

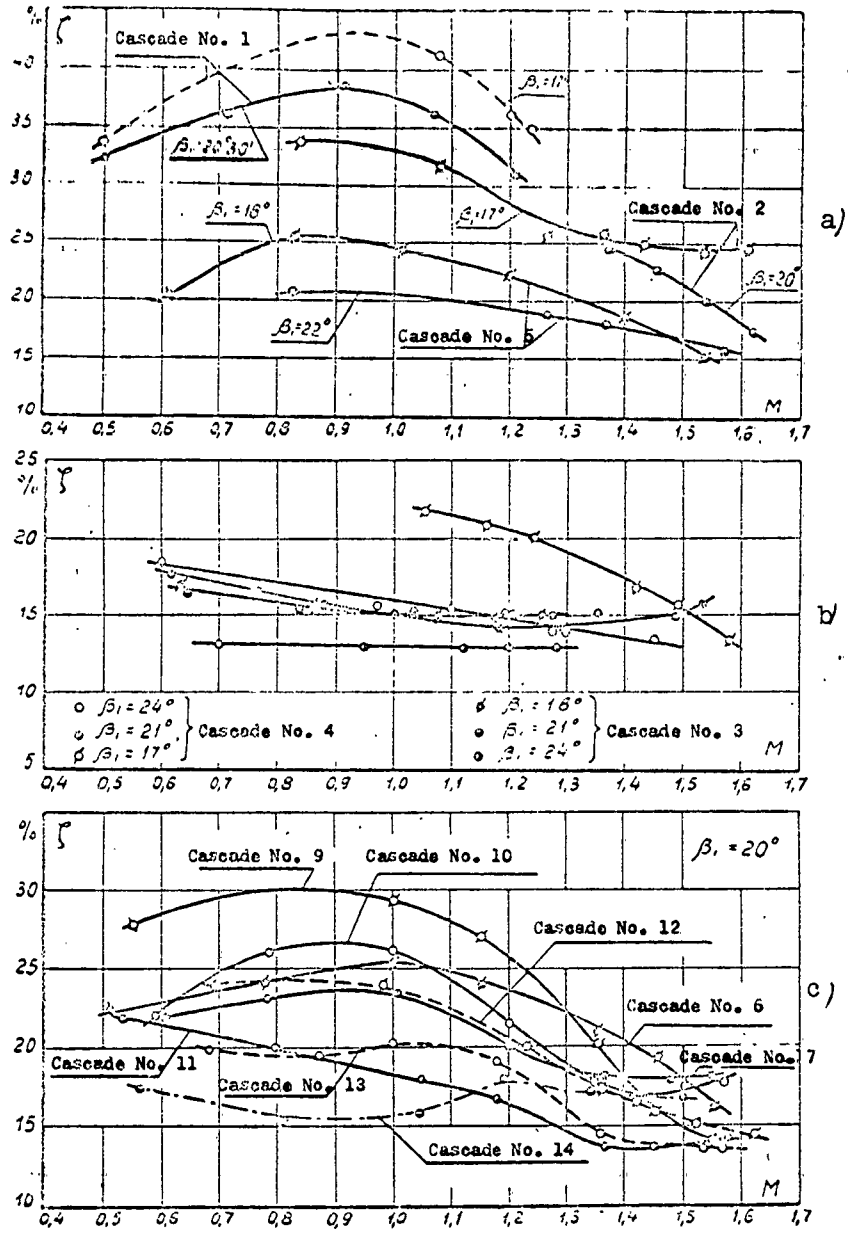

Fig. 3. Total losses in cascades vs. Mach number and flow-inlet angle: a) for type V cascades with a convergent-divergent vane channel; b) for type V cascades with slight divergence of the vane channel at the outlet; c) for modified TR-1V airfoil cascades, and type VS cascades.

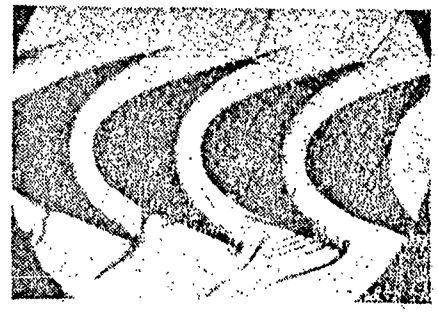

Fig. 4. The spectra of flow in cascades: a) cascade No. 8, M = 1.68, $\beta_1 = 22^\circ 30'$; b) cascade No. 9, M = 1.69, $\beta_1 = 22^\circ 30'$; c) cascade No. 12, M = = 1.67, $\beta_1 = 22^\circ 30'$.

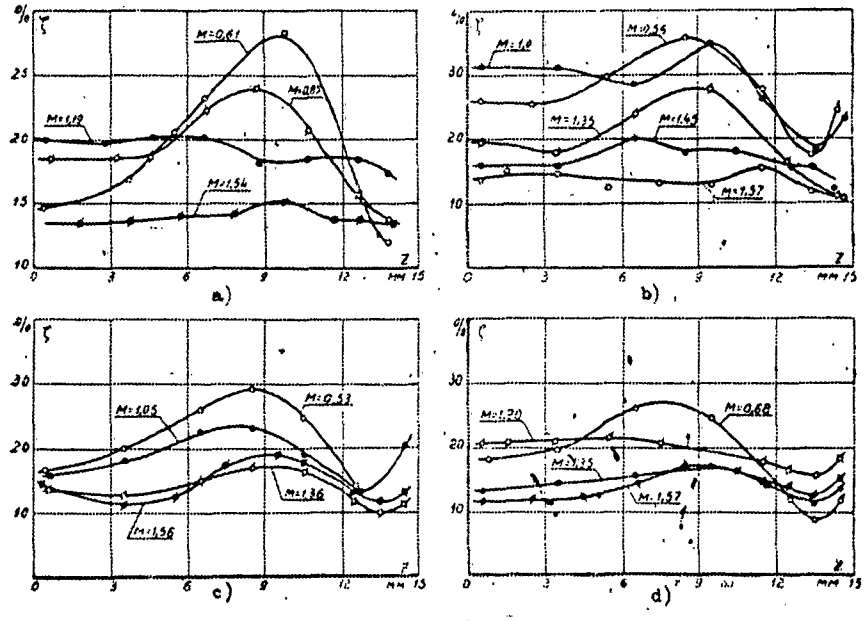

Fig. 5. Loss distribution along the height of the cascade: a) cascade No. 4, b = 15 mm, $\beta_1 = 21^\circ$; b) cascade No. 9, b = 20 mm, $\beta_1 = 20^\circ$; c) cascade No. 11, b = 20 mm, $\beta_1 = 20^\circ$; d) cascade No. 13, b = 20 mm, $\beta_1 = 20^\circ$.

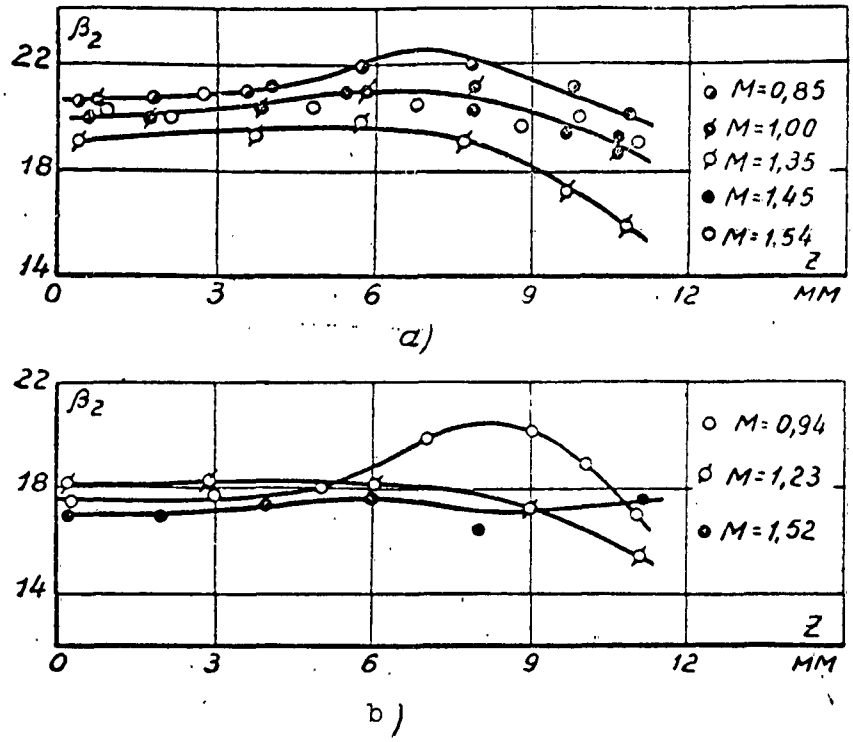

Fig. 6. Distribution of flow-outlet angles along the height of the cascade: a) cascade No. 4, b = 15° mm, $\beta_1 = 21°$; b) cascade No. 12, b = 20 mm, $\beta_1 = 20°$.

REFERENCES

1. A. V. Gubarev. Issledovaniye rabochikh reshetok osevykh turbin pri bol'shikh skorostyakh. Dissertatsiya, MEI, 1958.

2. M. Ye. Deych. Tekhnicheskaya gazodinamika. Gosenergoizdat, 1953.

3. K. Oswatisch. Allgemeine Wärmetechnik, No. 1, 1955.

4. Sh. Kh. Bikbulatov. "Aviatsionnaya Tekhnika," No. 2, 1958.

5. A. V. Gubarev and M. Ye. Deych. "Nauchnyye doklady vysshey shkoly," "Energetika," No. 2, 1958.

6. M. Ye. Deych and A. V. Gubarev. "Teploenergetika," No. 12, 1960.

7. M. Ye. Deych et al. "Teploenergetika," No. 5, 1955.

8. M. Ye. Deych and A. V. Gubarev. "Teploenergetika," No. 12, 1958.

AN APPROXIMATION METHOD FOR CALCULATING STEADY-STATE UNIFORM GAS FLOW IN A TUBE WITH EQUILIBRIUM DISSOCIATION AND IONIZATION, TAKING INTO ACCOUNT RESISTANCE AND HEAT TRANSFER

I. I. Suksov

At high temperatures we must take into account gas dissociation and ionization, which greatly complicates the calculation of gas flow. For equilibrium processes the calculations are simplified considerably if we have tables of the thermodynamic functions. Such tables are available for air [1, 2]. The handbook "Physical Gasdynamics" [3] contains, in addition to the theoretical bases for the compilation of these tables, the solution of certain gasdynamic problems for dissociated and ionized air. Individual problems of gasdynamics, taking into account the influence of dissociation and ionization of the air, have been treated previously [4].

On the basis of the tables [1, 2] data have been obtained from a calculation of one-dimensional isentropic air flow with equilibrium dissociation and ionization [12].

In this work we give an approximate graphoanalytic method which makes it possible to calculate one-dimensional isentropic flow in

tubes, i.e., to take into account the influence of resistance and heat transfer.

Yu. I. Balakleyevskiy helped in the calculations used to develop this method.

1. An Approximate Solution to the Equations

Let us write the equations of steady-state one-dimensional movement of a viscous compressible gas in a tube during constant flow with removal of heat from the gas [5]:

flow equation:

$$Fg\rho w = G = \text{const}, \tag{1.1}$$

energy equation:

$$Jgdh + wdw + Jgdq_a = 0, \tag{1.2}$$

equation of the first law of thermodynamics:

$$dq = dh - \frac{1}{Jg}\frac{dp}{\rho} = -\left(dq_a - \frac{1}{Jg}dl_r\right), \tag{1.3}$$

where F is the cross-sectional area of the tube (m^2); g is the acceleration of gravity (m/sec^2); ρ is the density ($kg\text{-}sec^2/m^4$); w is the velocity (m/sec); G is the weight flow (kg/sec); I = 427 kg-m/kcal is the mechanical equivalent of heat; h is the enthalpy (kcal/kg); dq is the elementary amount of heat (kcal/kg); dq_a is the elementary amount of heat released from 1 kg of gas (kcal/kg); p is pressure (kg/m^2); and dl_r is the elementary work of drag (m^2/sec^2).

On the basis of (1.3) we get an equation for entropy s:

$$ds = -\frac{1}{T}\left(dq_a - \frac{1}{Jg}dl_r\right). \tag{1.4}$$

The value of dl_r is defined by the expression

$$dl_r = \zeta\frac{w^2}{2}\frac{dx}{D}, \tag{1.5}$$

where ζ is the resistance coefficient; $\underline{x}$ is the coordinate read along the tube axis (m); D is the tube diameter (m); for tubes of noncircular cross section, D is understood to be the hydraulic diameter.

The elementary heat

$$dq_a = q_w \frac{dF_\delta}{G}, \tag{1.6}$$

where

$$q_w = q_k + q_{rad}, \tag{1.7}$$

dF_δ is an area element of the side of the tube (m^2); q_w is heat flow to the wall (kcal/m^2sec); q_k is convective heat flow (kcal/m^2sec); and q_{rad} is radiation heat flow (kcal/m^2sec).

The following relations hold:

$$dF_\delta = 4F\frac{dx}{D}, \tag{1.8}$$

$$q_k = \alpha_h (h_1 - h_w), \tag{1.9}$$

$$\alpha_h = g\rho w C_h, \tag{1.10}$$

$$q_{rad} = 0{,}001361\,\varepsilon'_{wall}\left[\varepsilon\left(\frac{T}{100}\right)^4 - A\left(\frac{T_w}{100}\right)^4\right], \tag{1.11}$$

where α_h is the local heat-transfer coefficient (kg/m^2sec); $\varepsilon_{wall} = 0.5(1 + \varepsilon_{wall})$; $C_h = q_w/q_\rho{}^w(h_i - h_w)$ is the local Stanton number; ε_{wall} is the degree of blackness of the wall; ε is the degree of blackness of the gas at temperature T; A is the absorptivity of the gas at temperature T_w (assumed equal to the value of ε at temperature T_w). The subscripts "i" and "w" indicate conditions of a heat-insulated and cooled wall, respectively.

Taking into account (1.5)-(1.11) we get for dq_a and ds the expressions

$$dq_a = \left\{4(h_1 - h_w)C_h + 0{,}005444\,\varepsilon'_{wall}\left[\varepsilon\left(\frac{T}{100}\right)^4 - A\left(\frac{T_w}{100}\right)^4\right]\frac{1}{g\rho w}\right\}\frac{dx}{D}, \tag{1.12}$$

$$ds = \frac{1}{T}\left(dq_a - \frac{\zeta}{2fg}w^2\cdot\frac{dx}{D}\right). \tag{1.13}$$

The enthalpy h_1 is defined by the formula

$$h_i = h + r_h \frac{w^2}{2g}, \tag{1.14}$$

where r_h is the recovery factor.

Let us examine the problem of determining the velocity w, temperature T, pressure p, and density ρ of a high-temperature gas in cross sections of a tube in presence of dissociation and ionization, considering these processes to be equilibrium processes. The starting data are: gas flow G, temperature T_{00} and pressure p_{00} of isentropic stagnation in cross section $x = x_0$, and also the geometry of the tube. In addition, we should know the dependences of the dimensionless values ζ, r_h, and C_h on the similarity parameters; the degree of blackness of the gas ε; the degree of blackness of the surface of the tube walls ε_{wall}; and we should have the distribution of enthalpy or temperature on the wall for the length of the tube.

As will be shown, with tables of the thermodynamic functions similar to those for air [1, 2], the problem can be solved relatively simply by means of graphoanalysis.

Using Eqs. (1.1), (1.2), (1.4), and (1.5), the system of equations for the given problem can be written:

$$w = \sqrt{2lg}\sqrt{h_{00} - h - \Delta h}, \tag{1.15}$$

$$s = s_{00} - \Delta s, \tag{1.16}$$

$$G = \gamma w F, \tag{1.17}$$

$$w = aM, \tag{1.18}$$

where $\gamma = g\rho$; a is the speed of sound;

$$\Delta h = \int_{x_0}^{x} dq_a, \quad \Delta s = \int_{x_0}^{x} \frac{1}{T}\left(dq_a - \frac{\zeta w^2}{2lg} \cdot \frac{dx}{D}\right). \tag{1.19}$$

The value of dq_a is determined from (1.12). The subscript "00" indicates, as before, stagnation parameters when $x = x_0$.

Let us first examine flow without resistance and heat transfer ($dl_r = dq_a = 0$), i.e., isentropic flow.

For this case, Eqs. (1.15)-(1.18) assume the form

$$w = \sqrt{2lg}\,\sqrt{h_{00} - h}, \tag{1.20}$$

$$s = s_{00} = \text{const}, \tag{1.21}$$

$$F = \frac{G}{\gamma}, \tag{1.22}$$

$$w = aM. \tag{1.23}$$

Knowing T_{00} and p_{00} let us determine, from the tables of thermodynamic functions, the enthalpy h_{00} and the entropy s_{00}. For a number of values of pressure $p < p_{00}$ and when $s = s_{00}$, we determine, from the tables, the corresponding values of temperature T, enthalpy h, speed of sound a, and the value of γ. Using Eq. (1.20) let us construct a graph of w vs. h; using (1.23) let us construct w vs. h for a number of given values of M (a set of curves). The intersection of the curves determines the values of w and h corresponding to the selected M values. Then (graphically or by interpolation using the tables) we determine the desired values of T, p, and ρ, and from Formula (1.22) we calculate the values of the cross-sectional area F (if p is given, we determine the flow from (1.22)).

The solution for isentropic flow is the first approximation when solving the problem of gas flow in a tube.

This method just examined differs somewhat from that used previously [12]. We note that the graphic data [12] in many cases are sufficient to determine all the parameters of isentropic air flow and for a logical division of the tube into parts in order to take into account the influence of resistance and heat transfer.

Now let us examine the solution of Eqs. (1.15)-(1.18) for the general case. Let us divide the tube into parts and examine the k-th section. The values at the beginning and end of this section will be designated by the subscripts (k-1) and k, respectively.

On the basis of Eqs. (1.15)-(1.18) we have

$$w_k = \sqrt{2lg}\sqrt{h_{0,\,k-1} - h_k - \Delta h_k}, \tag{1.24}$$

$$s_k = s_{k-1} - \Delta s_k, \tag{1.25}$$

$$w_k = \frac{G}{\gamma_k F_k}, \tag{1.26}$$

$$M = \frac{w_k}{a_k}, \tag{1.27}$$

where $h_{0,k-1} = h_{k-1} = w_{k-1}^2/2lg$ is stagnation enthalpy in the (k-1)-th section,

$$\Delta h_k = \int_{x_{k-1}}^{x_k} dq_a, \quad \Delta s_k = \int_{x_{k-1}}^{x_k} \frac{1}{T}\left(dq_a - \frac{\zeta w^2}{2lg}\frac{dx}{D}\right), \tag{1.28}$$

where dq_a is taken on the basis of (1.12).

The integrals in each section are defined approximately by the system

$$I_k = \int_{x_{k-1}}^{x_k} \Phi_k dx \approx \Phi_{k\text{am}}\,\Delta x, \tag{1.29}$$

where the subscript "am" indicates the taking of the arithmetic mean.

$$\Delta x = x_k - x_{k-1}.$$

Using the known parameters in the (k-1)-th section, the gas parameters in the k-th section are determined as follows.

First we find the gas parameters in the k-th section, considering that the flow in the examined section is isentropic (these parameters are given the subscript "ki"). Knowing the parameters with the subscripts "k-1" and "ki" let us calculate the integrals according to system (1.29); let us determine the entropy s_k according to (1.25). Assigning, when $s = s_k$, several test values to p_k close to p_{ki} and determining h_k and γ_k by interpolation of the tables, we calculate the corresponding values of w_k from Formulas (1.24) and (1.26) (the values of F_k are the same as those obtained earlier for isentropic flow). Let us construct the curves $w_k = f_1(h_k)$ and $w_k = f_2(h_k, F_k)$; the intersection

of these curves gives the desired values of w_k and h_k. Then we determine the parameters T_k, p_k, a_k, and ρ_k, and calculate the number M from (1.27). Thus is calculated flow in a tube, beginning with the first section.

In this calculation method, as the thermodynamic magnitudes which uniquely define all parameters of gas flow in a tube, we selected enthalpy h and entropy s. Let us note that it becomes ambiguous to determine the gas parameters using total enthalpy h_0 ane entropy $s = s_0$ in the case of isentropic flow.

2. Data for Approximate Evaluations

When using this approximation calculation method we must know, as has been said, the dependences of the values ζ, r_h, and C_h on the similarity parameters, and the dependence of the degree of blackness of the gas ε on temperature, pressure, and path length for the dissociated gas. As far as we know, there are no such data for tubes. For effusers and tubes of constant cross section, in particular for nozzles and the working part of thermal wind tunnels, we can consider that the resistance is exhausted by friction, i.e.,

$$\zeta = 4c_f, \tag{2.1}$$

where $c_f = 2\tau_w/\rho w^2$ is the local friction factor, and τ_w is frictional stress on the wall (kg/m^2).

In these cases, if the boundary layer occupies a small portion of the cross section, the use of rules of friction and heat transfer for a flat plate in the calculations will give a good approximation. However, even for a flat plate we do not have available systematized data on friction and heat transfer for a sufficiently broad range of changes in the similarity criteria.

To obtain approximate evaluations of the influence of convection heat transfer and friction we can, until more reliable data are forthcoming, use formulas in which account is taken of the variability of the physical parameters across the boundary layer and the basic effect of dissociation [6].

For a laminar boundary layer

$$c_{fw} \cdot \mathrm{Re}_w^{0,5} = 0{,}664 \left(\frac{\mu_* \rho_*}{\mu_w \rho_w}\right)^{\frac{1}{3}} \cdot \left(\frac{\mu \rho}{\mu_w \rho_w}\right)^{\frac{1}{15}\frac{h_w}{h_i}}, \tag{2.2}$$

$$C_{hw}\,\mathrm{Re}_w^{0,5} = 0{,}332\,\mathrm{Pr}_w^{-\frac{2}{3}} \left(\frac{\mu_* \rho_*}{\mu_w \rho_w}\right)^{\frac{1}{3}} \left(\frac{\mu \rho}{\mu_w \rho_w}\right)^{\frac{1}{15}\frac{h_w}{h_i}}, \tag{2.3}$$

where

$$c_{fw} = \frac{2\tau_w}{\rho_w w^2},\quad C_{hw} = \frac{q_w}{g\rho w\,(h_i - h_w)},\quad \mathrm{Re}_w = \frac{\rho_w w x}{\mu_w},$$

h_i is determined from Formula (1.14) where $r = 0.84$ and $\mathrm{Pr}_w = 0.71 = \mathrm{const}$. For a turbulent boundary layer

$$c_{fw}\,\mathrm{Re}_w^{0,2} = 0{,}058 \left(\frac{h_w}{h_i}\right)^{0,39} \cdot (1 + 0{,}2rM^2)^{0,11}, \tag{2.4}$$

$$C_{hw}\mathrm{Re}_w^{0,2} = 0{,}029\,P_{rw}^{-0,6} \left(\frac{h_w}{h_i}\right)^{0,39} \cdot (1 + 0{,}2rM^2)^{0,11}, \tag{2.5}$$

where $r = 0.89$. The function $h(T)$ is given in Fig. 1.

The subscript "*" indicates parameters pertaining to maximum enthalpy in boundary layer $\underline{h}$, whereupon we have the relation

$$\frac{h_* - h_w}{h_0 - h_w} = 0{,}25\,\frac{1 + \omega - \frac{h_w}{h_i}}{\omega};\quad h_0 = h + \frac{w^2}{2lg};\quad \omega = \frac{w^2}{2lgh}. \tag{2.6}$$

Exceptions to this formula: if $\omega \leq 1 - h_w/h$, $h_* = h$; if $h_w/h_0 \geq 1$, $h_* = h_w$.

The formulas for the transition from c_{fw} and C_{hw} to c_f and C_h:

$$c_f = \frac{\rho_w}{\rho}\,c_{fw},\quad C_h = \frac{\rho_w}{\rho}\,C_{hw}.$$

Figure 2 gives the coefficient of viscosity μ vs. $\underline{h}$ for $T \leq 1873^\circ K$. When $T > 200^\circ K$ we can use the familiar graphic function $\mu(T, P)$ [11].

Let us note that the last term in (2.2) and (2.3) can be disregarded because of the small exponent.

We should bear in mind that the approximate nature of data on convection heat transfer and friction introduce no noticeable error into the flow parameters, since the estimated influence is relatively slight, even in a turbulent regime.

The values of ε_{wall} necessary for calculating radiation heat transfer are familiar for a great many materials [7, 8]. The accessible literature contains no data on the degree of blackness of a gas ε at temperatures higher than 2000°K. For temperatures $T < 2000$°K we have data on gas radiation [7], in which is noted the negligible radiation absorptivity of monatomic and diatomic gases. We also know [9] that at low pressures ($p < 0.1$ atm) the role of atmospheric radiation in the general heat balance is slight, even at very high temperatures (8000-10,000°K). From physical concepts it follows that with increasing pressure and increasing beam path length the radiation absorptivity of a gas increases [7], i.e., its degree of blackness increases, tending toward a limiting value $\varepsilon = 1$ for an absolutely black body. Such conditions can be realized, e.g., with high-voltage arc discharge; then it is assumed that the arc radiates as an absolutely black body [10].

3. Calculation Results

To extimate the combines influence of convection heat transfer, radiation, and friction we calculated the air friction in a section of a round cylindrical tube with diameter d = 20 mm and length l = 50 mm ($l/d = 2.5$). The flow regime was assumed to be turbulent. We used the following data: stagnation temperature and pressure in the initial section T_{00} = 12,000°K, p_{00} = 200 atm; M = 1; cooled-wall temperature

T_w = 900°K; the value $0.5(1 + \varepsilon_{wall}) \approx 1$; degree of blackness of the air $\varepsilon \approx 1$. The section was not divided into parts, since the tube was cylindrical and the ratio l/d was small. After determining the parameters of isentropic flow we calculated the drop in total enthalpy Δh and entropy Δs from the formulas

$$\Delta h = \Delta h_k + \Delta h_{rad}, \quad \Delta s = \frac{\Delta h_k + \Delta h_{rad} - \Delta h_{mp}}{T},$$

$$\Delta h_k = 0{,}116\, \mathrm{Pr}_w^{-0.6} \frac{\rho_w}{\rho} \left(\frac{h_w}{h_1}\right)^{0.39} \mathrm{Re}_{w\,am}^{-0.2} (1 + 0{,}2rM^2)^{0.11} (h_1^! - h_w) \frac{l}{d},$$

$$\Delta h_{rad} = 0{,}00544 \left(\frac{T}{100}\right)^4 \frac{1}{\gamma w} \frac{l}{d},$$

$$\Delta h_f = 0{,}116 \frac{\rho_w}{\rho} \left(\frac{h_w}{h_1}\right)^{0.39} \mathrm{Re}_{w\,am}^{-0.2} (1 + 0{,}2rM^2)^{0.11} \frac{w^2}{lg} \frac{l}{d}.$$

The derived working formulas or Δh_k, Δh_{rad}, and Δh_f were obtained on the basis of relations (1.12), (1.19), (2.1), (2.4), (2.5), and (2.7). When calculating Δh_{rad} the term $A(T_w/100)^4$ was discarded.

We obtained the following values: Δh_k = 514, Δh_{rad} = 390, Δh_f = = 67, Δh = 904, Δs = 0.0758.

Then, using the given method we determined the flow parameters at the end of the tube.

Figure 3 and 4 gives the graphic determination of the parameters w, h, T, p, and ρ for isentropic flow and at the end of the tube, respectively (the velocities w_1 were calculated from (1.20) and (1.24)).

The table gives the calculation results.

This example of a calculation shows that heat transfer and friction can have a substantial influence on the parameters of the flow of a high-temperature gas in a tube. This can happen, e.g., in the initial sections of nozzles of supersonic hyperthermal tubes.

Submitted September 18, 1961

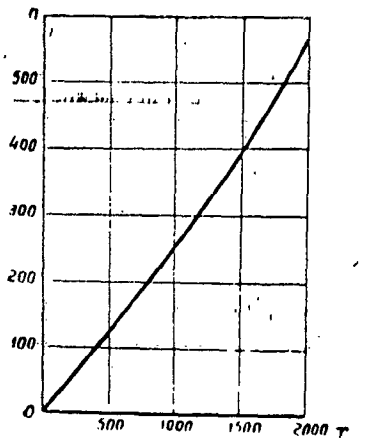

Fig. 1.

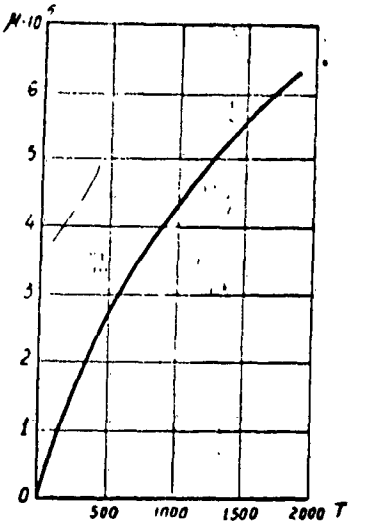

Fig. 2.

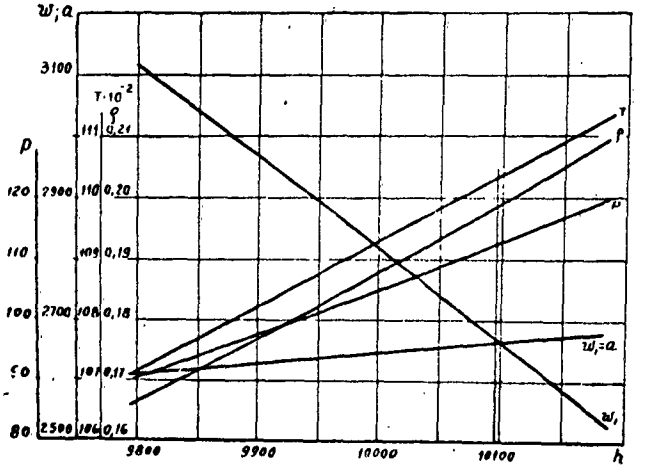

Fig. 3.

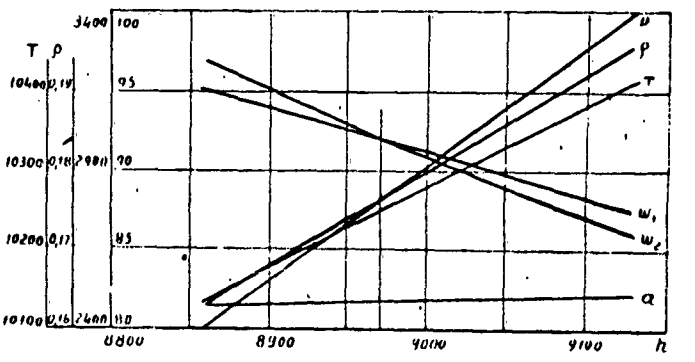

Fig. 4.

Type of flow	h_0	s	h	w	T	p	a	ρ	M
Isentropic	10950	3,309	10096	2665	11040	112,5	2665	0,1989	1
With friction and heat transfer	10046	3,233	8972	3000	10250	88,2	2492	0,1764	1,204

REFERENCES

1. A. S. Predvoditel'yev et al. Tablitsy termodinamicheskikh funktsiy vozdukha (dlya temperatur ot 6000 do 12000°K i davleniy ot 0.001 do 1000 atmosfer). Izd. AN SSSR, Moscow, 1957.

2. A. S Predvoditel'yev et al. Tablitsy termodinamicheskikh funktsiy vozdukha (dlya temperatur ot 12000 do 20000°K i davleniy ot 0.001 do 1000 atmosfer). Izd. AN SSSR, Moscow, 1959.

3. Fizicheskaya gazodinamika. Sbornik energeticheskogo instituta AN SSSR, Izd. AN SSSR, Moscow, 1959.

4. I V. Nemchinov. Uchet vliyaniya dissotsiatsii i ionizatsii vozdukha v nekotorykh zadachakh gazovoy dinamiki. Sbornik "Issledovaniya po mekhanike i prikladnoy matematike," Trudy Moskovskogo fiziko-tekhnicheskogo instituta, No. 1, 1958.

5. L. A Vulis. Termodinamika gazovykh potokov. Gosenergoizdat, M-L, 1950.

6. V. S. Avduyevskiy et al. Osnovy teploperedachi v aviatsionnoy i raketnoy tekhnike. Oborongiz, Moscow, 1960.

7. M. A. Mikheyev. Osnovy teploperedachi. Gosenergoizdat, M-L, 1949.

8. I. I. Drakin. Aerodinamicheskiy i luchistyy nagrev v polete. Oborongiz, Moscow, 1961.

9. L. Lees. Heat-transfer processes on entry of a vehicle into dense layers of the atmosphere. Technical translation No. 9973 (in Russian), Institut im. Zhukovskogo, 1960.

10. G. A. Sisoyan. Elektricheskaya duga v elektricheskoy pechi. Metallurgizdat, Moscow, 1961.

11. V. A. Bashkin and Ye. Ye. Solodkin. Rashet laminarnogo pogranichnogo sloya pri otsutstvii prodol'nogo gradienta davleniya i v okrestnosti kriticheskoy tochki tela s uchetom termokhimicheskikh reaktsiy, protekayushchikh v gaze pri vysokikh temperaturakh. Trudy Instituta im. Zhukovskogo, No. 777, Moscow, 1960.

12. V. Ya. Borovoy and V. L. Yakusheva. Atlas statsionarnykh odnomernykh techeniy vozdukha s ravnovesnoy dissotsiatsiyey i ionizatsiyey. Institut im. Zhukovskogo, 1961.

DISTRIBUTION LIST

DEPARTMENT OF DEFENSE	Nr. Copies
HEADQUARTERS USAF	
AFCIN-3D2	1
ARL (ARB)	1
OTHER AGENCIES	
CIA	1
NSA	6
DIA	9
AID	2
OTS	2
AEC	2
PWS	1
NASA	1
ARMY (FSTC)	3
NAVY	3
NAFEC	1
RAND	1
PGE	12

MAJOR AIR COMMANDS	Nr. Copies
AFSC	
SCFDD	1
DDC	25
TDBTL	5
TDBDP	5
TDEPA (Boehme)	1
TDEPA (Van Dame)	1
AEDC (AEY)	1
SSD (SSF)	2
ASD (ASYIM)	1
AFFTC (FTY)	1
AFSWC (SWF)	1
BSD (BSF)	1